Available online at www.sciencedirect.com
SCIENCE DIRECT®

International Journal of Refrigeration 29 (2006) 645–658

REVUE INTERNATIONALE DU FROID
INTERNATIONAL JOURNAL OF
refrigeration

www.elsevier.com/locate/ijrefrig

# A comprehensive design and rating study of evaporative coolers and condensers. Part I. Performance evaluation

Bilal A. Qureshi, Syed M. Zubair*

*Mechanical Engineering Department, KFUPM Box #1474, King Fahd University of Petroleum and Minerals, Dhahran 31261, Saudi Arabia*

Received 10 November 2004; received in revised form 17 August 2005; accepted 20 September 2005

Available online 15 December 2005

**Abstract**

The mathematical models of evaporative fluid coolers and evaporative condensers are studied in detail to perform a comprehensive design and rating analysis. The mathematical models are validated using experimental as well as numerical data reported in the literature. These models are integrated with the fouling model presented in an earlier paper, using the experimental data on tube fouling. In this paper, we use the fouling model to investigate the risk based thermal performance of these evaporative heat exchangers. It is demonstrated that thermal effectiveness of the evaporative heat exchangers degrades significantly with time indicating that, for a low risk level ($p = 0.01$), there is about 66.7% decrease in effectiveness for the given fouling model. Furthermore, it is noted that there is about 4.7% increase in outlet process fluid temperature of the evaporative fluid cooler. Also, a parametric study is performed to evaluate the effect of elevation and mass flow rate ratio on typical performance parameters such as effectiveness for rating calculations while surface area for design calculations.


*Keywords:* Refrigeration; Air conditioning Cooling tower; Evaporative condenser; Modelling; Heat transfer; Mass transfer; Performance

# Etude approfondie et évaluation des tours de refroidissement et condenseurs évaporatifs. Partie. I. Evaluation de la performance

*Motsclés :* Froid ; Conditionnement d'air ; Tour de refroidissement ; Condenseur évaporatif ; Modélisation ; Transfet de Chaleur ; Transfert de masse ; Performance

## 1. Introduction

The phenomenon of cooling by evaporation is well known and it has found many industrial applications. A rational development of a combined cooling-tower heat-exchanger unit is the evaporative fluid cooler and evaporative condenser. In these heat exchangers, the purpose of the cooling tower is to cool water, and of the heat exchanger, to cool the process fluid using the cooled water, is merged. It is important to note that, with the growth of the refrigeration and air conditioning industry, the evaporative cooler came into extensive use, principally, as a refrigerant condenser. Fig. 1 shows a combined schematic diagram of the evaporative fluid cooler and evaporative condenser. In case of the former, fluid flows from the bottom

* Corresponding author. Tel.: +966 3 860 3135; fax: +966 3 860 2949.

*E-mail address:* smzubair@kfupm.edu.sa (S.M. Zubair).

0140-7007/$35.00 © 2005 Elsevier Ltd and IIR. All rights reserved.
doi:10.1016/j.ijrefrig.2005.09.014

**Nomenclature**

| | |
|---|---|
| $A$ | outside surface area of cooling tubes ($m^2$) |
| $a$ | interfacial area per unit volume of a tube bundle ($m^2\ m^{-3}$) |
| $C_1$ | represents increase in performance index as fouling reaches its asymptotic value |
| $C_2$ | constant used in asymptotic fouling model (Eq. (2)) |
| $c_p$ | specific heat at constant pressure (kJ $kg^{-1}\ C^{-1}$) |
| $d$ | diameter (m) |
| $E$ | slope of the tie-line ($E=-U_{os}/h_D$) (kJ $kg^{-1}\ C^{-1}$) |
| $f_D$ | friction factor |
| $g$ | gravitational acceleration (m $s^{-2}$) |
| $h$ | specific enthalpy (kJ $kg^{-1}$) |
| $h_c$ | convective heat-transfer coefficient (kW $m^{-2}\ C^{-1}$) |
| $h_D$ | convective mass-transfer coefficient ($kg_w\ m^{-2}\ s^{-1}$) |
| $h_f$ | specific enthalpy of saturated liquid water (kJ $kg_w^{-1}$) |
| $h_{f,w}$ | specific enthalpy of water evaluated at $t_w$ (kJ $kg_w^{-1}$) |
| $h_g$ | specific enthalpy of saturated water vapor (kJ $kg_w^{-1}$) |
| $h_g^0$ | specific enthalpy of saturated water vapor evaluated at 0 °C (kJ $kg_w^{-1}$) |
| $h_{fg,w}$ | change-of-phase enthalpy ($h_{fg,w}=h_{g,w}-h_{f,w}$) (kJ $kg_w^{-1}$) |
| $k$ | thermal conductivity (kW $m^{-1}\ C^{-1}$) |
| $L$ | length of tube (m) |
| $Le$ | Lewis factor ($Le=h_c/h_D c_{p,a}$) |
| $M$ | median thickness to reach critical level of fouling |
| $\dot{m}$ | mass flow rate of fluid (kg $s^{-1}$) |
| $m_{ratio}$ | water-to-air mass flow rate ratio ($m_{ratio}=\dot{m}_{w,in}/\dot{m}_a$) |
| $n_{tr}$ | number of tube rows |
| NTU | number of transfer units |
| $Nu$ | Nusselt number |
| $p$ | risk level |
| $P$ | pressure (kPa) |
| $\widehat{P}$ | pitch (m) |
| $Pr$ | Prandtl number |
| $\dot{Q}$ | heat transfer (kW) |
| $R_f$ | fouling resistance (C $kW^{-1}$) |
| $R_f''$ | fouling resistance per unit area, ($m^2$ C $kW^{-1}$) |
| $R_{int}$ | interface resistance (C $kW^{-1}$) |
| $Re$ | Reynolds number |
| $t$ | temperature (°C); time (s) |
| $U$ | overall heat transfer coefficient, (kW $m^{-2}\ C^{-1}$) |
| w.r.t. | with respect to |
| $W$ | humidity ratio of moist air ($kg_w\ kg_a^{-1}$) |
| $\eta_Q$ | cooler/condenser performance index |
| $\sqrt{\alpha}$ | scatter in time |
| $\Phi^{-1}$ | inverse of the cumulative normal distribution function |
| $\phi$ | rate of deposition or removal of fouling material ($m^2$ C $kJ^{-1}$) |
| $\delta$ | thickness (mm) |
| $\varepsilon$ | effectiveness |
| $\Gamma$ | water flow rate per unit tube length (kg $m^{-1}\ s^{-1}$) |
| $\mu$ | dynamic viscosity (kg $m^{-1}\ s^{-1}$) |
| $\rho$ | density (kg $m^{-3}$) |
| *Subscripts* | |
| a | air |
| atm | at atmospheric conditions |
| c | condensate |
| cl | clean conditions |
| cal | calculated |
| cr | critical fouled conditions |
| d | deposition |
| da | dry air |
| db | dry-bulb |
| ec | evaporative condenser |
| efc | evaporative fluid cooler |
| f | final value |
| fl | fouled conditions |
| F | fill |
| g,w | vapor at water temperature |
| i | initial value |
| in | inlet |
| int | air-water interface |
| is | inside |
| norm | normalized |
| os | outside |
| out | outlet |
| p | process fluid |
| r | removal; refrigerant |
| s,w | saturated moist air at water temperature |
| t | tube |
| tot | total |
| v | vapor |
| w | water |
| wb | wet-bulb |

to top and in case of the latter, the refrigerant flows from the top to bottom.

The modeling of an evaporative cooler or condenser is complicated by the fact that three fluids, normally flowing in different directions, interact with each other through heat and mass transfer processes. Many modeling procedures, each with a varying degree of approximation, can be found in the literature [1–3]. The evaporative condenser models developed in these papers assumed a constant spray water temperature. This assumption is also typically employed in

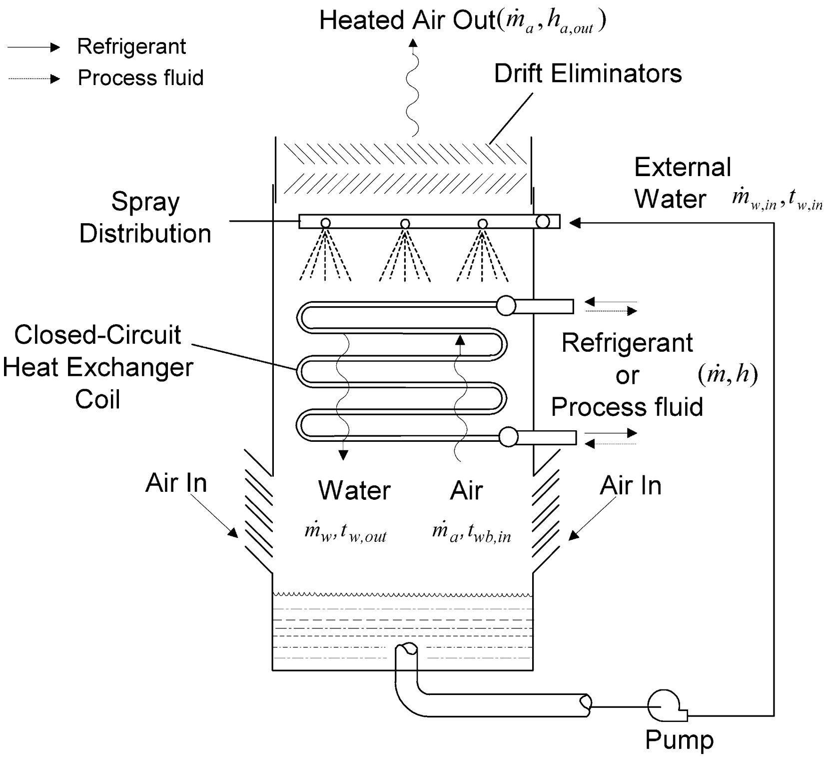


Fig. 1. Combined schematic of a counter-flow evaporative fluid cooler and evaporative condenser.

evaporative cooler models as well. Parker and Treybal [4] realized that this assumption caused the mathematical equations of the model to become inconsistent, thus, giving a meaningless answer. They reported a detailed experimental study to define the heat and mass transfer coefficients in the fluid cooler. Leidenfrost and Korenic [5] followed a development in their model similar to that of Parker and Treybal and demonstrated that the numerical solutions for proper design can only be obtained by iterative techniques. It was also shown by experiments that the amount of water sprayed onto a coil to produce complete wetting is sufficient for maximum performance of the condenser. Dreyer [6] presented various mathematical models for thermal evaluation of evaporative coolers and condensers. These models ranged from the exact model based on Poppe [7] to the simplified models of Mizushina et al. [8,9]. Zalewski and Gryglaszewski [10] developed a mathematical model for evaporative fluid coolers based on the model of an evaporative condenser proposed by Zalewski [11]. The model took into account the effect of heat and mass transfer area between air and water on the heat flux in the heat exchanger in dependence of the structure of the water flow down across the tubes. Alonso et al. [12] developed a universal heat and mass transfer model based on basic principles that could be used to analyze different indirect evaporative cooler designs and conditions. On the other hand, Halasz [13] developed a general non-dimensional model applicable to all types of evaporative devices, which required substituting the real saturation line with a straight one. For each device, a unique rating procedure could be established conveniently as it was irrespective of the relative flow direction of the fluids involved.

Mizushina et al. [9] developed two different rating methods for evaporative coolers; one, a numerical technique and the other, a simpler analytical model based on the assumption of constant water temperature. Finlay and Grant [14] showed that the assumption of constant water temperature might lead to errors in excess of 30 percent, for example, in large tube banks. A rating method, based on cooling tower procedures, was proposed by Tezuka et al. [15] but the assumptions made in this model were not as accurate as those used in the model of Parker and Treybal or in the simple model of Mizushina. In another report, Finlay and Grant [16] simplified the equations describing the mass transfer in an evaporative cooler by assuming that the vapor pressure of saturated moist air is a linear function of temperature. The model is generally considered to be very accurate, as this is the only major assumption made in the derivation. The final design equations are very complicated, however, and require a numerical solution.

Webb [17] performed a unified theoretical treatment for thermal analysis of cooling towers, evaporative condensers and evaporative fluid coolers. In this paper, specific calculation procedures are outlined for sizing and rating

each type of evaporative heat exchanger. The author explained that the 'tie-line' is a line of slope $E=(h_{a,int}-h_a)/(t_{int}-t_p)$ that intersects the saturated air enthalpy curve (evaluated at the interface temperature) and the operating line at ($h_a$, $t_p$). It was also stated that the value of the tie-line is a constant for an evaporative condenser but varies along the air path in the evaporative fluid cooler. In another paper, Webb and Villacres [18] describe three computer algorithms that have been developed to perform rating calculations of three evaporatively cooled heat exchangers. The algorithms are particularly useful for rating commercially available heat exchangers at off-design conditions. Bykov et al. [19] investigated the heat and mass transfer and fluid flow characteristics in an evaporative condenser and found a complex pattern of water temperature and air enthalpy change. Their research facilitated optimizing the heat and mass transfer spaces as well as the effect of extended surfaces. On the other hand, the optimization of the geometrical and operating parameters of an evaporative fluid cooler was presented by Zalewski et al. [20]. Guo and Zhao [21] numerically analyzed the thermal performance of an indirect evaporative air cooler and showed that a smaller channel width, a lower inlet relative humidity of the secondary air stream, a higher wettability of the plate, and a higher velocity ratio of the secondary air to the primary air stream gave a higher effectiveness. However, these authors did not discuss the impact of fouling on the performance of these evaporative heat exchangers.

The objective of this paper is to present a risk based (or probabilistic) approach to the analysis of a fouling model that we presented in an earlier paper and to depict its impact on thermal performance of evaporative coolers and condensers. In this regard, we present evaporative cooler and condenser models, in conjunction with the fouling model. These models are used to study the effect of fouling on thermal performance parameters such as effectiveness when operating under similar operating conditions.

## 2. Fouling growth model

The most widely accepted fouling model, which is used in conventional heat exchangers, is based on the material balance equation first proposed by Kern and Seaton [22]:

$$\frac{dR_f(t)}{dt}=\phi_d-\phi_r \tag{1}$$

In the above equation, the rate of fouling deposition, $\phi_d$, depends on the type of fouling mechanism (sedimentation, crystallization, organic material growth, etc.), while the rate of fouling removal, $\phi_r$, depends on both the hardness and adhesive strength of the deposit and the shear stress due to the flow velocity, as well as the coil configuration. The rates of deposition and removal have been given many different forms in the heat exchanger literature (depending upon the type of fouling mechanism) by various investigators.

In monitoring fouling in evaporative coolers and condensers, the increase in thickness (due to net effect of deposition and removal processes) with respect to time is not difficult to ascertain on any site. Thickness gives a good indication of the tube bank tendencies with regard to fouling, but does not directly address the users' main interest; that is, performance degradation due to coil fouling. The users of these heat exchangers are mainly interested in knowing; (i) correlation between the thickness and fouling, (ii) loss in thermal performance, (iii) the effect of foulant thickness on pressure drop, and normalized performance index. Qureshi and Zubair [23], using the experimental fouling data reported in Macleod-Smith [24] have recently developed a model similar to the one presented in [25]. The model demonstrates a correlation between normalized cooler/condenser performance index ($\eta_{Q,norm}$) due to fouling as a function of thickness $\delta$. The model is of the form [23]

$$\eta_{Q,norm}=\frac{(\dot{Q}_{cl}-\dot{Q}_{fl})}{\dot{Q}_{cl}}=C_1\left(1-\exp\left(\frac{-\delta}{C_2}\right)\right) \tag{2}$$

where $C_1$ and $C_2$ are constants depending on the fouling characteristics of the evaporative fluid cooler or evaporative condenser. $C_1$ represents the increase in value of $\eta_{Q,norm}$ when the fouling reaches its asymptotic value, and $C_2$ represents the thickness constant indicating that the performance index has decreased to 63.2% of the asymptotic value due to fouling. A linear description of the above model can be expressed as

$$\ln\left(\frac{1}{1-\frac{\eta_{Q,norm}}{C_1}}\right)=\frac{\delta}{C_2} \tag{3}$$

The constant $C_2$ is expressed in terms of the critical acceptable value of the cooler/condenser performance index $\eta_{Q,norm}$ as

$$C_2=\frac{\delta_{cr}}{\ln[1/(1-\eta_{Q,norm,cr}/C_1)]} \tag{4}$$

where the critical value of foulant thickness $\delta_{cr}$, is expressed as

$$\delta_{cr}=\frac{M}{[1-\sqrt{\alpha}\Phi^{-1}(p)]} \tag{5}$$

substituting Eqs. (4) and (5) in to Eq. (3) and simplifying, we get

$$\eta_{Q,norm}(\delta,p;\sqrt{\alpha}) = C_1[1-\exp\{-\ln[1/(1-\eta_{Q,norm,cr}/C_1)][1 - \sqrt{\alpha}\Phi^{-1}(p)](\delta/M)\}] \tag{6}$$

It should be noted that in the above equation, the risk level, $p$, represents the probability of the tubes being fouled up to a critical level after which cleaning is needed. The parameters $M$ and $\sqrt{\alpha}$ here represented the median thickness

and the scatter parameter in a transformed coordinate system, where the exponential fouling growth model may be treated as a linear replica. An illustration of the model represented in Eq. (6) is shown in Fig. 2, wherein the *y*-axis is transformed to represent a linear model of the heat exchanger performance index for various levels of risk factors.

## 3. Mathematical model of evaporative coolers and condensers

Fig. 3 shows a combined infinitesimal control volume of the basic model for evaporative fluid coolers and evaporative condensers. For both the evaporative fluid cooler and evaporative condenser, the air (subsystem I) is flowing in an upward direction whereas the water (subsystem II) is sprayed in a downward direction. It is considered that the process fluid (subsystem III) flows in the upward direction in an evaporative cooler while, in the case of an evaporative condenser, the refrigerant (subsystem III) flows downwards. The major assumptions that are used to derive the basic modeling equations may be summarized as [6,9,17]:

- The system is in steady state.
- The apparatus and the cooling water re-circulating circuit are insulated from the surroundings.
- Radiation heat transfer is ignored.
- Negligible water loss due to drift.
- The heat and mass transfer coefficients are constant within the tube bundle.
- Complete surface wetting of the tube bundle.
- The distribution of air and water is uniform at the inlets and this uniformity is maintained. Thus, the temperatures in the unit will only depend on the vertical position in the unit, which implies the model is one-dimensional.
- The film temperature at the air – water interface is equal to the bulk film temperature.
- The re-circulating water temperature at the inlet and outlet is same.
- The water film on the tubes is considered to be very thin i.e. the air – water interface area is approximately equal to the outer surface area of dry tubes.

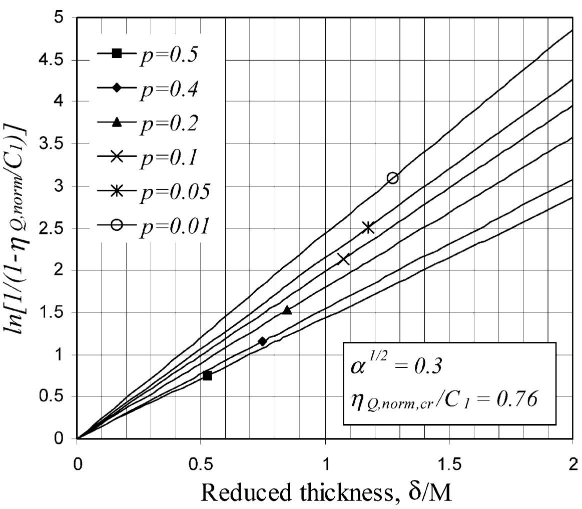


Fig. 2. Normalized cooler/condenser performance index versus reduced thickness ($\delta/M$) in the transformed coordinate system.

We see from Fig. 3 that the water mass balance, for both the evaporative cooler and condenser, can be written as

$$\dot{m}_a W + \dot{m}_w + \left(\frac{\partial \dot{m}_w}{\partial A}\right) dA = \dot{m}_w + \dot{m}_a \left[W + \left(\frac{\partial W}{\partial A}\right) dA\right] \quad (7)$$

After simplification, we get

$$\frac{\partial W}{\partial A} = \frac{1}{\dot{m}_a}\frac{\partial \dot{m}_w}{\partial A} \quad (8)$$

For both types of heat exchangers, the mass flow rate of the recirculating water evaporating into the air, in terms of the mass-transfer coefficient ($h_D$), is given by

$$\dot{m}_w + \left(\frac{\partial \dot{m}_w}{\partial A}\right) dA = \dot{m}_w + h_D(W_{s,int} - W) dA \quad (9)$$

Simplifying, we get

$$d\dot{m}_w = h_D(W_{s,int} - W) dA \quad (10)$$

It is obvious from Eqs. (8) and (10) that the water mass flow rate does not remain constant due to the process of evaporation.

For both the evaporative cooling devices, simultaneous heat and mass transfer takes place at the air–water interface that can be expressed as

$$\dot{m}_a \left[h_a + \left(\frac{\partial h_a}{\partial A}\right) dA\right] = \dot{m}_a h_a + h_c(t_{int} - t_a) dA + h_D(W_{s,int} - W) h_{fg,int} dA \quad (11)$$

Simplifying the above equation, introducing the Lewis factor, $Le = h_c/h_D c_{p,a}$, and assuming that $h_{fg} \approx h_g$ results in [6,23]

$$dh_a = \frac{h_D dA}{\dot{m}_a}[(h_{s,int} - h_a) + [Le - 1]\{(h_{s,int} - h_a) - (W_{s,int} - W) h_{g,int}\}] \quad (12)$$

where $c_{p,a}$ is the specific heat of the mixture and $h_{g,int}$ is specific enthalpy of water vapor evaluated at the interface temperature, $t_{int}$. If Lewis factor is taken as unity, we get

$$dh_a = \frac{h_D}{\dot{m}_a}(h_{s,int} - h_a) dA \quad (13)$$

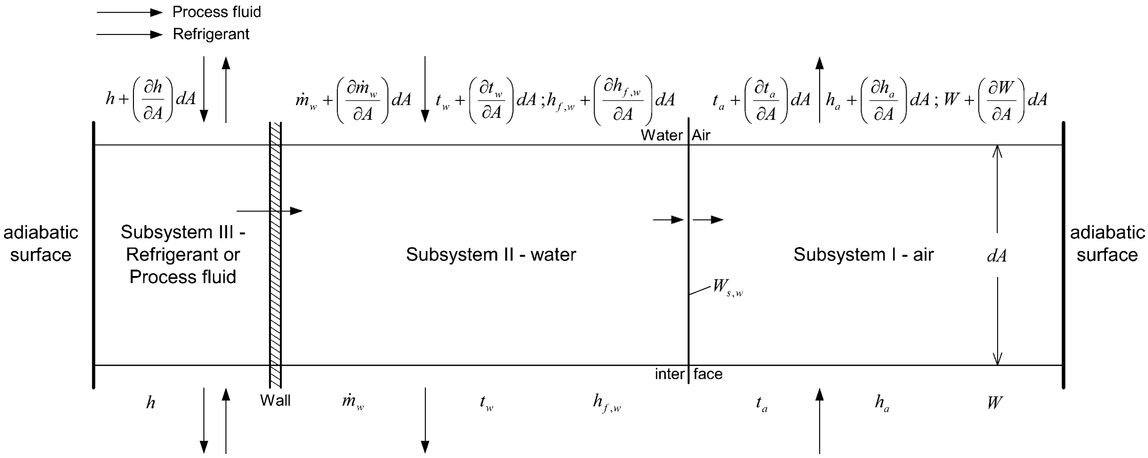


Fig. 3. Infinitesimal control volume of the basic model for an evaporative fluid cooler and evaporative condenser.

Now, let the enthalpies of the water and process fluid be written as

$$\frac{\partial h_{\mathrm{f,w}}}{\partial A} = c_{\mathrm{p,w}}\left(\frac{\partial t_{\mathrm{w}}}{\partial A}\right); \quad \frac{\partial h_{\mathrm{p}}}{\partial A} = c_{\mathrm{p,p}}\left(\frac{\partial t_{\mathrm{p}}}{\partial A}\right) \tag{14}$$

From Fig. 3, we see that the overall energy balance on the process fluid of the evaporative cooler can be written as:

$$\dot{m}_{\mathrm{p}} h_{\mathrm{p}} = \dot{m}_{\mathrm{p}}\left[h_{\mathrm{p}} + \left(\frac{\partial h_{\mathrm{p}}}{\partial A}\right)\mathrm{d}A\right] + U_{\mathrm{os}}(t_{\mathrm{p}} - t_{\mathrm{int}})\mathrm{d}A \tag{15}$$

Using Eq. (14) and simplifying, we get

$$\mathrm{d}t_{\mathrm{p}} = -\frac{U_{\mathrm{os}}}{\dot{m}_{\mathrm{p}} c_{\mathrm{p,p}}}(t_{\mathrm{p}} - t_{\mathrm{int}})\mathrm{d}A \tag{16}$$

and $U_{\mathrm{os}}$ is the time-dependent (due to fouling) overall heat transfer coefficient based on the outer area of the tubes.

The overall energy balance on the control volume (refer to Fig. 3) for the evaporative cooler results in

$$\dot{m}_{\mathrm{a}} h_{\mathrm{a}} + \left[\dot{m}_{\mathrm{w}} + \left(\frac{\partial \dot{m}_{\mathrm{w}}}{\partial A}\right)\mathrm{d}A\right]\left[h_{\mathrm{f,w}} + \left(\frac{\partial h_{\mathrm{f,w}}}{\partial A}\right)\mathrm{d}A\right] + \dot{m}_{\mathrm{p}} h_{\mathrm{p}} = \dot{m}_{\mathrm{a}}\left[h_{\mathrm{a}} + \left(\frac{\partial h_{\mathrm{a}}}{\partial A}\right)\mathrm{d}A\right] + \dot{m}_{\mathrm{w}} h_{\mathrm{f,w}} + \dot{m}_{\mathrm{p}}\left[h_{\mathrm{p}} + \left(\frac{\partial h_{\mathrm{p}}}{\partial A}\right)\mathrm{d}A\right] \tag{17}$$

Neglecting higher order terms, simplifying and using Eq. (14), we get

$$\mathrm{d}t_{\mathrm{w}} = \frac{1}{\dot{m}_{\mathrm{w}} c_{\mathrm{p,w}}}[\dot{m}_{\mathrm{a}}\mathrm{d}h_{\mathrm{a}} - c_{\mathrm{p,w}} t_{\mathrm{w}}\mathrm{d}\dot{m}_{\mathrm{w}} + \dot{m}_{\mathrm{p}} c_{\mathrm{p,p}}\mathrm{d}t_{\mathrm{p}}] \tag{18}$$

In the above equation, it is important to note that some of the heat removed from the process fluid goes to heating (or cooling) the water film.

Following a similar approach on the control volume of the evaporative condenser with regard to the overall energy balance, wherein the condensing fluid flows in a top to bottom direction (Figs. 1 and 3), we get

$$\mathrm{d}t_{\mathrm{w}} = \frac{1}{\dot{m}_{\mathrm{w}} c_{\mathrm{p,w}}}[\dot{m}_{\mathrm{a}}\mathrm{d}h_{\mathrm{a}} - c_{\mathrm{p,w}} t_{\mathrm{w}}\mathrm{d}\dot{m}_{\mathrm{w}} - \dot{m}_{\mathrm{r}}\mathrm{d}h_{\mathrm{r}}] \tag{19}$$

Applying a similar procedure to the evaporative condenser as was used previously to formulate Eq. (16), keeping in mind the direction of flow of the condensing fluid (refer to Figs. 1 and 3) as well as the fact that the refrigerant enthalpy changes but its temperature remains constant, we get

$$\mathrm{d}h_{\mathrm{r}} = \frac{U_{\mathrm{os}}}{\dot{m}_{\mathrm{r}}}(t_{\mathrm{r}} - t_{\mathrm{int}})\mathrm{d}A \tag{20}$$

The time-dependent conductance (UA) of the heat exchanger can be written as

$$\frac{1}{UA} = \frac{1}{h_{\mathrm{c,p}} A_{\mathrm{is}}} + \frac{\ln(d_{\mathrm{t,os}}/d_{\mathrm{t,is}})}{2\pi k_{\mathrm{t}} L} + \frac{1}{h_{\mathrm{c,w}} A_{\mathrm{os}}} + R_{\mathrm{int}} + R_{\mathrm{f}}(t) \tag{21}$$

It should be noted that

$$U_{\mathrm{os}} A_{\mathrm{os}} = U_{\mathrm{is}} A_{\mathrm{is}} = UA \tag{22}$$

Now, if the temperature of the interface film is considered the same as the bulk water temperature, then all the terms with the subscripts (s, int) will be replaced by (s, w) effectively reducing the interface thermal resistance to zero i.e. $R_{\mathrm{int}} \rightarrow 0$. And this is the approach that was used in the current work.

## 4. Numerical solution procedure

The full system of five differential equations describing the operation of the evaporative fluid cooler is given by Eqs. (8), (10), (13), (16) and (18); whereas the system of five differential equations describing the operation of the

evaporative condenser is given by Eqs. (8), (10), (13), (19) and (20). It should be noted that the correlations for convective and condensation heat transfer coefficients inside the tubes as well as the mass transfer and the film heat transfer coefficients outside the tubes are used from various sources which are summarized in the Appendix A.

A computer program is written in engineering equation solver (EES) for solving these equations for both the cooler and condenser. In this program, properties of air–water vapor mixture are needed at each step of numerical calculation, which are obtained from the built-in functions provided in EES. Each differential equation is first transformed into an appropriate form by integrating both sides. We then use EES to solve initial value differential equations as detailed below [26]:

In an evaporative fluid cooler, for the process fluid, we write

$$t_p = t_{p,in} + \int_{A_i}^{A} \left(\frac{dt_p}{dA}\right) dA \tag{23}$$

where the term in brackets is known from Eq. (16).

Similarly, for air and water, the other equations are written as follows:

$$h_a = h_{a,in} + \int_{A_i}^{A} \left(\frac{dh_a}{dA}\right) dA \tag{24}$$

$$t_w = t_{w,out} + \int_{A_i}^{A} \left(\frac{dt_w}{dA}\right) dA \tag{25}$$

$$W = W_{in} + \int_{A_i}^{A} \left(\frac{dW}{dA}\right) dA \tag{26}$$

$$\dot{m}_w = \dot{m}_{w,out} + \int_{A_i}^{A} \left(\frac{d\dot{m}_w}{dA}\right) dA \tag{27}$$

where the term in brackets for Eqs. (24)–(27) are known from Eqs. (13), (18), (8), and (10), respectively. In evaporative fluid coolers, the process fluid can be considered to be flowing from bottom-to-top or top-to-bottom. In this study, the former configuration was considered for comparatively easier calculation of results and, therefore, the process fluid temperature at the bottom ($t_{p,in}$) is known. It should be noted that air and water are flowing in a counter-current direction and that the integration is performed from bottom to top. Therefore, the recirculating water temperature and water mass flow rate at the bottom of the heat exchanger must be guessed through iterations. The correct water temperature ($t_{w,out}$) is the one, due to which, the water temperature at the top of the heat exchanger comes out to be the same as at the bottom. Similarly, the correct water flow rate at the bottom ($\dot{m}_{w,out}$) is the one, which gives the known value of the water flow rate at the inlet (i.e. at the top). The numerical solution for the evaporative condenser is performed in a similar manner.

The number of transfer units of the evaporative fluid cooler and condenser is calculated by

$$\frac{h_D A}{\dot{m}_a} = \int_{h_{a,in}}^{h_{a,out}} \frac{dh_a}{(h_{int} - h_a)} = \text{NTU} \tag{28}$$

It is important to note that the NTU is a measure of the air–water interface area required to affect the required heat transfer duty.

The effectiveness of the evaporative fluid cooler and condenser are defined as the ratio of actual energy to the maximum possible energy transfer from the fluid in the tubes and are given by the following two set of equations:

$$\varepsilon_{efc} = \frac{t_{p,in} - t_{p,out}}{t_{p,in} - t_{wb,in}} \tag{29}$$

$$\varepsilon_{ec} = \frac{h_{r,in} - h_{r,out}}{h_{r,in} - h_{wb,in}} \tag{30}$$

The effectiveness of the evaporative fluid cooler (Eq. (29)) is based on the fact that the lowest possible temperature achievable for the process fluid is the wet bulb temperature. Regarding the evaporative condenser (Eq. (30)), Ettouney et al. [27] explained that the maximum amount of heat removed from the condenser occurs as the condensate temperature cools to the wet bulb temperature of the air.

Calculations regarding the evaporative fluid cooler have been validated from the experimental data provided by Jang and Wang [28] shown in Fig. 4(a) and the results were found to be in good agreement. Fig. 4(b) and (c) show a comparison of evaporation prediction made by our evaporative fluid cooler and evaporative condenser models, respectively, and a procedure used by Baltimore Aircoil [29]. For the fluid cooler, the error ranged from −0.9 to 6% and from 1.4 to −14.8% for the condenser. Furthermore, numerical examples provided by other authors [12,14,30,31] were also compared with the values obtained by our model, and the results are summarized in Table 1. The percentage error in the calculated outlet process fluid temperature ($t_{p,out}$), evaluated from the present model, was found to be quite reliable (within ±2.25%). Similarly, experimental [5] as well as numerical data [6] were compared to validate the evaporative condenser model. It was noted that the percentage error in the calculated condenser temperature ($t_r$), evaluated from the present model using the experimental data provided by Leidenfrost and Korenic [5], was found to be acceptable (within ±5.6%). Also, the results of two numerical examples given by Dreyer [6] were also

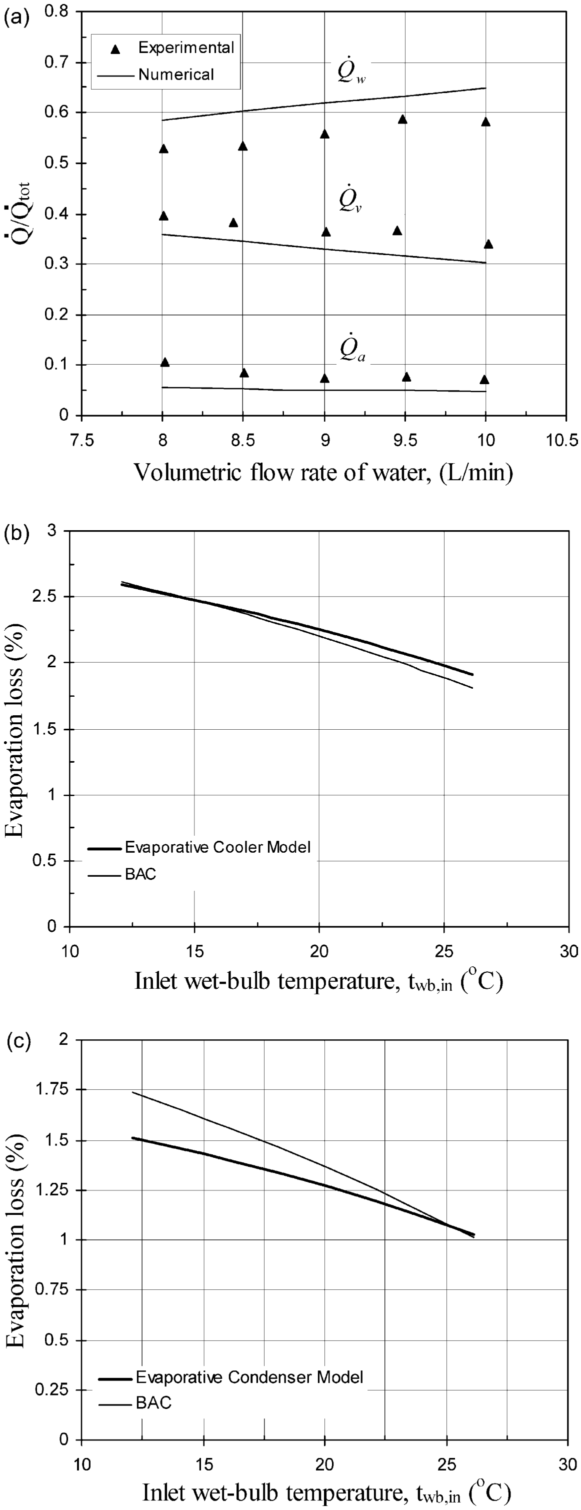


Fig. 4. (a) Verification of evaporative cooler model from the data of Jang and Wang [28]. (b) Comparison of evaporation loss in evaporative fluid cooler. (c) Comparison of evaporation loss in evaporative condenser.

compared and the errors associated with the heat transfer prediction were found to be less than 2.2%.

## 5. Effect of fouling on thermal performance

The mathematical model of the evaporative cooler and condenser discussed in the previous section can be used for design and rating calculations of these class of heat exchangers. It should be noted that the rating calculations procedure is used for studying the effect of fouling on evaporative cooler and condenser performance. In rating calculations, parameter such as process fluid outlet temperature ($t_{p,out}$) and effectiveness ($\varepsilon_{efc}$) are calculated for the following set of input conditions: inlet air temperatures [dry bulb ($t_{db,in}$) and wet bulb ($t_{wb,in}$)], process fluid inlet temperature ($t_{p,in}$) or condenser temperature($t_r$), mass flow rates [air ($\dot{m}_a$), water ($\dot{m}_{w,in}$) and process fluid ($\dot{m}_p$) or refrigerant ($\dot{m}_r$)], performance index ($\eta_Q$) and tube surface area ($A$). While in design calculations, the tube surface area is calculated for the following set of input conditions: inlet air temperatures (dry bulb and wet bulb temperatures), process fluid inlet and outlet temperatures, ($t_{p,in}$, $t_{p,out}$), mass flow rates [air ($\dot{m}_a$), water ($\dot{m}_{w,in}$) and process fluid ($\dot{m}_p$) or refrigerant ($\dot{m}_r$)] and performance index ($\eta_Q$).

The evaporative cooler and condenser models, in combination with the fouling model, are used for studying thermal performance under fouled conditions. The time dependent effectiveness of the evaporative cooler and condenser discussed in an earlier section are presented in Fig. 5(a) and 6(a) in a reduced coordinate system. Fig. 5(a) is drawn for the following set of input data: $t_{db,in}=25$ °C, $t_{wb,in}=18$ °C, $t_{p,in}=50$ °C, $A=9.111$ m$^2$, $Le=1$, $\dot{m}_{w,in}=2.5$ kg/s, $\dot{m}_a=2.913$ kg/s and $\dot{m}_p=6$ kg/s while Fig. 6(a) is drawn for: $t_{db,in}=25$ °C, $t_{wb,in}=18$ °C, $t_r=50$ °C, $A=9.703$ m$^2$, $Le=1$, $\dot{m}_{w,in}=2.666$ kg/s, $\dot{m}_a=1.88$ kg/s and $\dot{m}_r=0.1086$ kg/s, where ammonia was used as the refrigerant. In these figures, reduced effectiveness $\varepsilon(\delta, p; \sqrt{\alpha})/\varepsilon(0)$ versus reduced fouling thickness $\delta/M$ plots for different risk levels $p$, representing the probability of the tube surface being fouled up to a critical level after which a cleaning is needed; and scatter parameter $\sqrt{\alpha}=0.3$, are plotted for the fouling-growth model that we presented earlier. As expected, the effectiveness of the evaporative cooler and condenser degrade significantly with time indicating that for a low risk level ($p=0.01$), there is about 66.7% decrease in effectiveness for the given fouling model, when $\delta/M=1.0$. The variations in the reduced process fluid outlet temperature versus reduced fouling thickness for different risk levels $p$ and for scatter parameter $\sqrt{\alpha}=0.3$, is shown in Fig. 5(b). As one would expect, the figures show that for a low risk level (i.e. high reliability) when compared with the deterministic case, the process fluid outlet temperature is high, indicating that there will be a lower heat transfer rate due to fouling compared with the deterministic case. It is

noticed that there is about 4.7% increase in the fluid outlet temperature for the given fouling model. The same percentage decrease in heat transfer is observed for the evaporative condenser as can be seen from Fig. 6(b).

We may notice from the above discussion that fouling reduces the thermal performance, which is reflected in the decreased value of the effectiveness. In order to achieve a constant value of the effectiveness, under fouled conditions, its surface area has to be increased. Figs. 7 and 8 show a plot of the area fraction ($A_{fl}/A_{cl}$) of the heat exchanger for different assumed values of $C_1$ for the evaporative cooler and condenser, respectively. The required surface area increases non-linearly in both cases. Also, it can be seen from the figure that the effect of atmospheric pressure (elevation) is insignificant.

## 6. Effect of atmospheric pressure (elevation)

Sutherland [32] mentioned that an increase in altitude of approximately 850 m would result in 10 kPa decrease of atmospheric pressure. This change in atmospheric pressure would definitely effect the operations of evaporative coolers and condensers because it directly influences the wet-bulb temperature. The wet bulb temperature is, theoretically, the lowest temperature that the process fluid can achieve and, therefore, it is important to quantify this effect, in terms of design, on required surface area to achieve a prescribed amount of cooling. Fig. 9(a) and (b) are drawn for the following set of input data that is also considered in Mizushina et al. [8]: $t_{db,in}=29$ °C, $t_{wb,in}=21.1$ °C, $t_{p,in}=50$ °C, $\dot{m}_p=0.325$ kg/s.

Fig. 9(a) shows the plot of the surface area required to achieve the necessary cooling of the process fluid versus the atmospheric pressure. The figure shows that for achieving the same fluid outlet temperature, the surface area of the tubes can be reduced by 0.3 m$^2$ when atmospheric pressure reduces by 17 kPa for $m_{ratio}=\dot{m}_{w,in}/\dot{m}_a=0.5$. As in the cooling tower [25], the reduction in required surface area with the increasing altitude occurs because both the dry and wet bulb temperatures decrease. Less surface area is needed for the same amount of cooling because the colder air comparatively cools the water better. Also, Eq. (16) shows

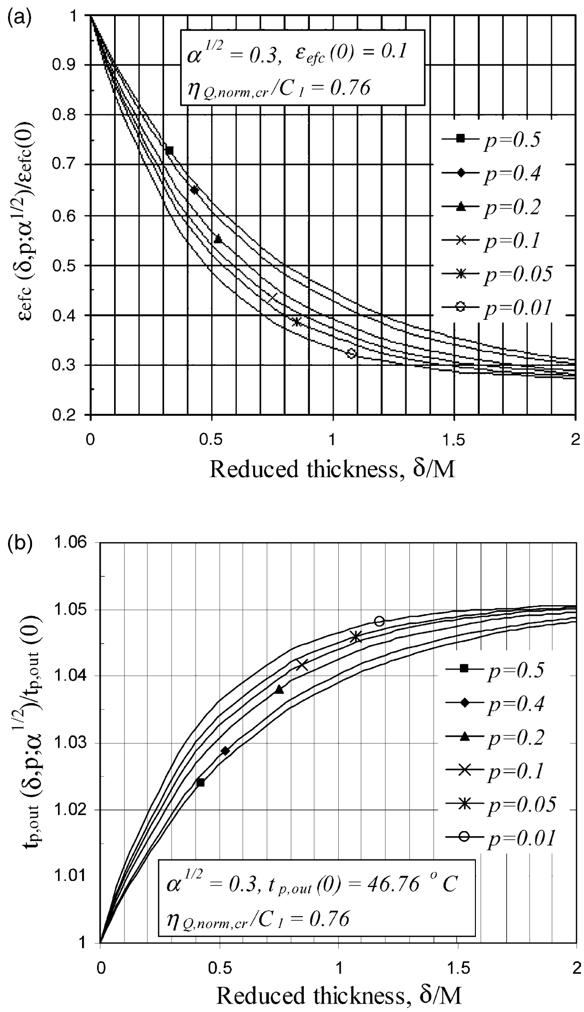


Fig. 5. Normalized efficiency (a) normalized outlet process fluid temperature (b) versus reduced thickness.

that, as the atmospheric pressure decreases, the value of $(t_p-t_w)$ increases due to the decreasing water temperature and, thus, the required surface area decreases. Now, the surface area is larger as the mass flow rate ratio decreases and is due to higher water temperatures achieved at these

Table 1
Percentage error in calculated values of outlet process fluid temperature

| $\dot{m}_a$ (kg/s) | $\dot{m}_{w,in}$ (kg/s) | $\dot{m}_p$ (kg/s) | $t_{db,in}$ (°C) | $t_{wb,in}$ (°C) | $t_{p,in}$ (°C) | $t^{ref}_{p,out}$ (°C) | $t^{calc}_{p,out}$ (°C) | $t_{p,out}$ (% error) |
|---|---|---|---|---|---|---|---|---|
| 1.880 | 2.667 | 15.00 | 25.0 | 19.50 | 50.0 | 48.32[a] | 48.11 | −0.414 |
| 0.166 | 0.458 | 0.325 | 17.5 | 13.43 | 44.8 | 37.50[b] | 37.58 | 0.213 |
| 2.070 | 1.845 | 2.670 | 10.0 | 8.450 | 15.6 | 13.55[c] | 13.55 | 0 |
| 2.913 | 2.500 | 6.000 | 25.0 | 18.00 | 50.0 | 44.15[d] | 45.14 | 2.242 |

[a] Dreyer [6].
[b] Mizushina and Miyashita [8].
[c] Finlay and Harris [30].
[d] Erens [31].

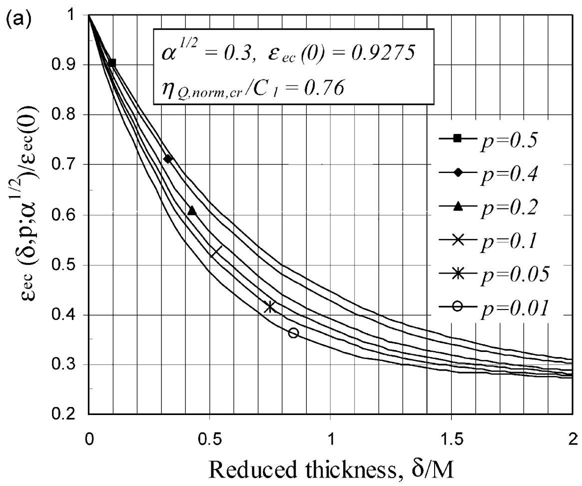


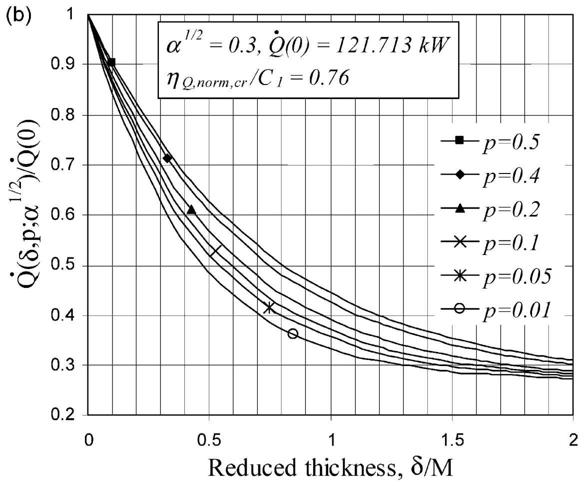


Fig. 6. Normalized efficiency (a) normalized load (b) versus reduced thickness.

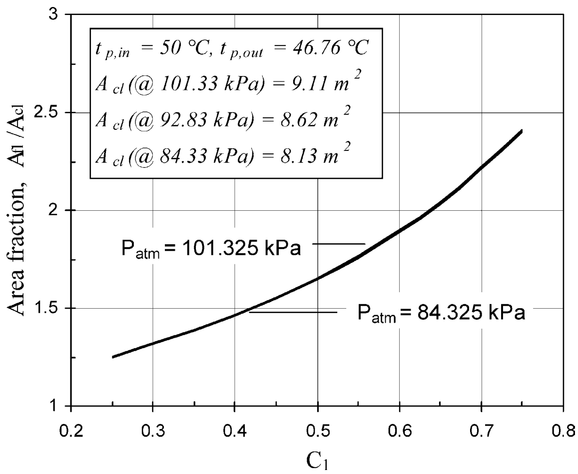


Fig. 7. Area fraction as a function of $C_1$ in evaporative fluid cooler.

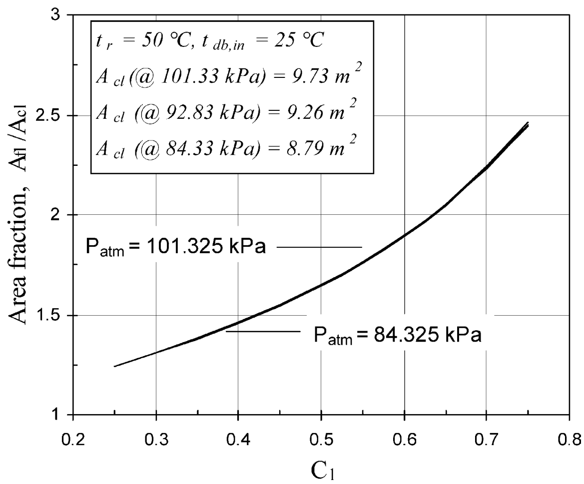


Fig. 8. Area fraction as a function of $C_1$ in evaporative condenser.

mass flow rate ratios (refer to Eqs. (16) and (18)). However, it is evident from Fig. 9(b) that the percentage decrease in the required surface area, with respect to the surface area calculated at standard atmospheric pressure, is almost the same for each value of $m_{ratio}$.

Since the evaporative cooler and condenser are very similar, it is not surprising that Fig. 10(a) and (b) are very similar to its counterpart evaporative cooler plots. These are drawn for the following set of input data that is also considered in Leidenfrost and Korenic [5]: $t_{db,in} = 29$ °C, $t_{wb,in} = 21.1$ °C, $t_r = 44.6$ °C, $\dot{m}_r = 0.013194$ kg/s, $\dot{m}_r = 0.06194$ kg/s. Fig. 10(a) shows that, to meet the heat load of the condensing refrigerant, the surface area of the tubes can be reduced by 0.042 m$^2$ when the atmospheric pressure varies from 101.325 tso 84.325 kPa at $m_{ratio} = \dot{m}_{w,in}/\dot{m}_a = 0.5$. The reasons for the reduction in the required surface are the same as in the case of the cooling tower [25] and evaporative cooler. Also, Eq. (20) shows that, as the atmospheric pressure decreases, the value of $(t_r - t_w)$ increases due to the decreasing steady-state water temperature and, thus, the required surface area decreases. Now, the surface area is larger as the mass flow rate ratio decreases and is due to higher water temperatures achieved at lower mass flow rate ratios (refer to Eqs. (19) and (20)). However, it can be seen from Fig. 10(b) that the percentage decrease in the required surface area, with respect to the surface area calculated at standard atmospheric pressure, is the same for each value of the mass flow rate ratio, similar to what we have seen earlier in the evaporative fluid cooler.

## 7. Effect of mass flow rate and the tie line

The water to air mass flow ratio ($m_{ratio} = \dot{m}_{w,in}/\dot{m}_a$) is an important factor and affects all aspects of the performance of the evaporative coolers and condensers as seen in the results already shown. Figs. 11 and 12 show the variation of the

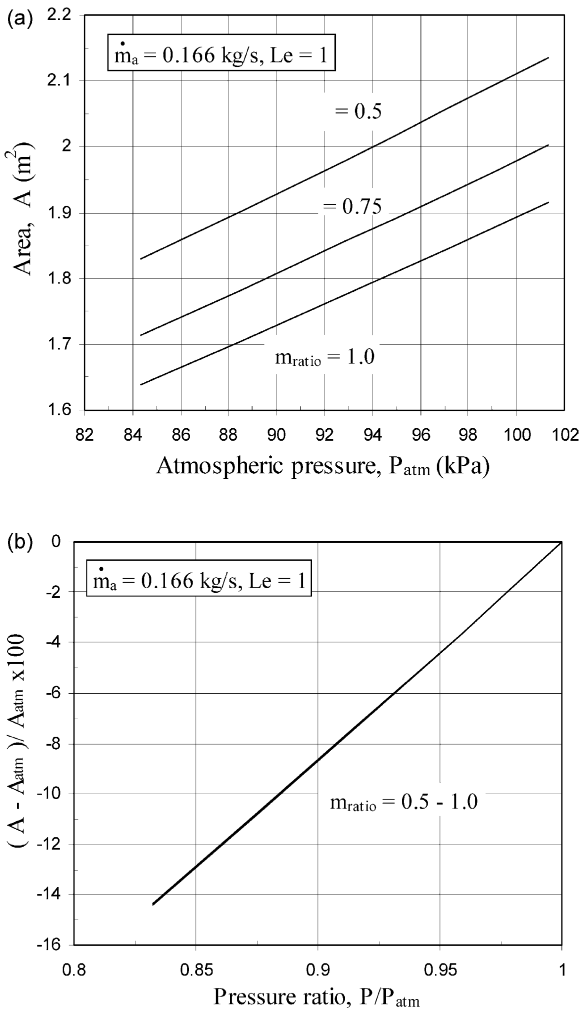


Fig. 9. Variation in required surface area (a) and percentage decrease in required surface area (b) versus atmospheric pressure, $P_{atm}$ in an evaporative cooler.

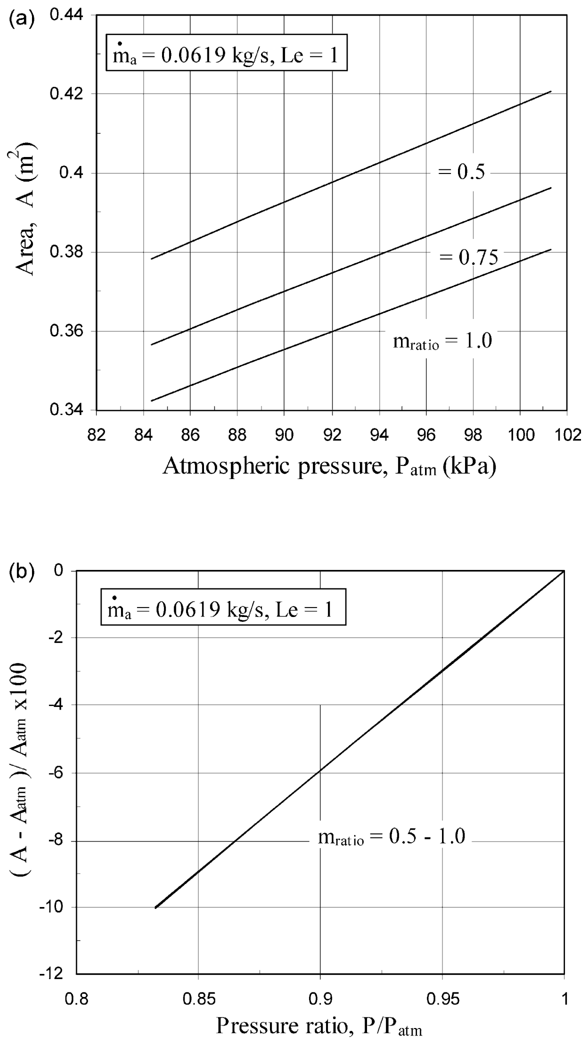


Fig. 10. Variation in required surface area (a) and percentage decrease in required surface area (b) versus atmospheric pressure, $P_{atm}$ in an evaporative condenser.

effectiveness in the typical range of the mass flow rate ratio for the evaporative cooler and condenser, respectively, wherein it increases for higher mass flow ratios due to higher values of the overall heat transfer coefficient obtained. The input data used was the same as that for all the previous evaporative cooler and condenser results. The steady-state water temperature acquired by the system in each case does not amount to a significant change over the whole range investigated and can be considered negligible (as shown in Table 2).

The variation of the tie-line ($E = -U_{os}/h_D$) was calculated in an evaporative cooler and condenser for a mass flow ratio of 1. It was found that the value of the tie-line was almost constant for the evaporative condenser and was found to be around $-8.8$; however, this variation was comparatively large ($-11.21$ to $-8.22$) in the evaporative cooler. Therefore, it was beneficial to evaluate the error in NTU-estimation assuming the value of the tie-line to be constant for the evaporative cooler in order to ascertain whether a representative value can be found. Fig. 13 is a plot between NTU and $E$ for the evaporative cooler where the latter was varied between the range found above. The error in calculating the NTU varied from $-13.8$ to 0.39%, which is quite large at one end. By considering the variation of E during the process, we found NTU $= 0.939$. This corresponds to a representative value of $E = -11.1$ as shown in the figure. It is worth noting that this is the same value that Baker and Shryok [33] found to yield the best results for cooling towers.

## 8. Concluding remarks

Evaporative cooler and condenser models are investigated by using engineering equation solver (EES) program,

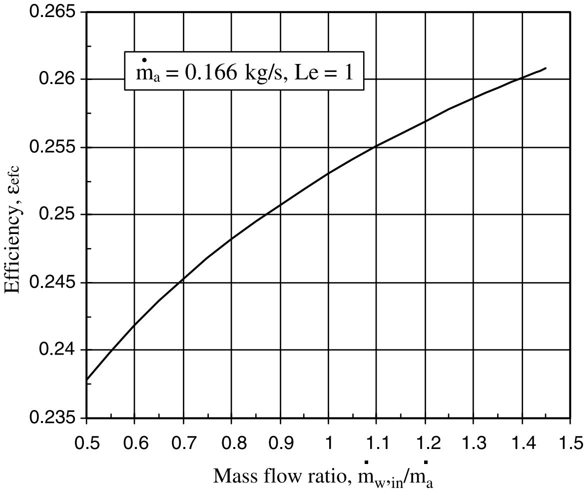


Fig. 11. Variation of effectiveness with mass flow ratio in an evaporative cooler.

which are validated with experimental as well as numerical data reported in the literature. An asymptotic fouling model, similar to the one developed for cooling towers, in conjunction with the numerical model of the counter flow evaporative cooler and condenser have been used to study the risk based performance characteristics of evaporative coolers and condensers, including the effect of fouling on the performance index. It is demonstrated that there is over 50% decrease in effectiveness for both the evaporative cooler and condenser. Furthermore, it is found that there is about 5% increase in the process fluid outlet temperature for the given fouling model. This also demonstrates the generality of the fouling model in that it not only applies to evaluating the performance of cooling towers but also of evaporative coolers and condensers.

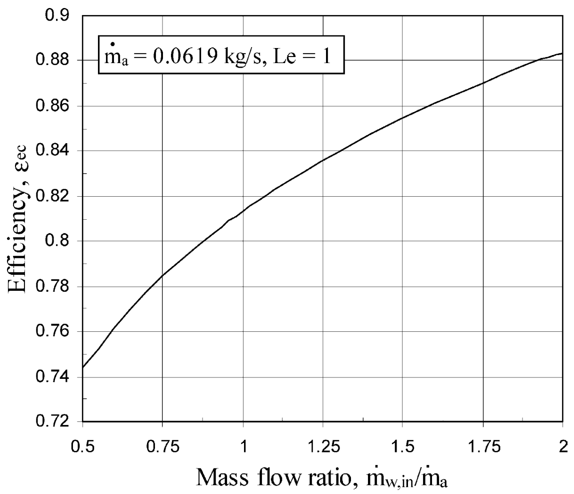


Fig. 12. Variation of effectiveness with mass flow ratio in an evaporative condenser.

Table 2
Water temperatures achieved for Figs. 11 and 12

| $m_{\text{ratio}}$ | $t_{w,efc}$ (°C) | $t_{w,ec}$ (°C) |
|---|---|---|
| 0.50 | 40.35 | 36.86 |
| 0.70 | 40.31 | 37.00 |
| 0.90 | 40.26 | 37.10 |
| 1.10 | 40.21 | 37.17 |
| 1.30 | 40.16 | 37.22 |

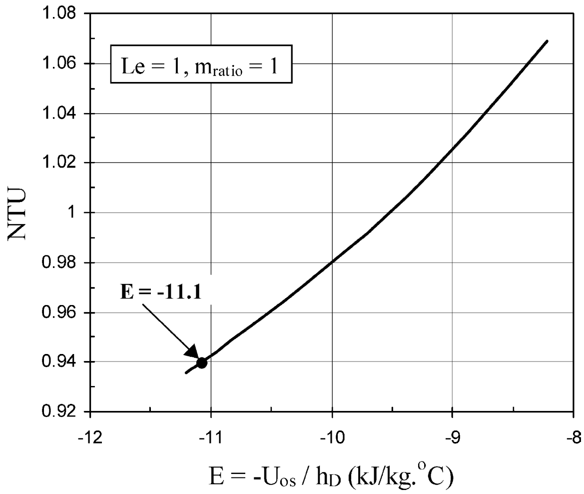


Fig. 13. NTU variation for different values of the tie-line ($E = -U_{os}/h_D$) in an evaporative fluid cooler.

An example problem is also presented for both cases wherein it is demonstrated that surface area of the tubes has to be increased in order to achieve the targeted thermal performance under fouled conditions whereas the atmospheric pressure does not have a significant effect. Furthermore, the effect of elevation on evaporative heat exchanger design is investigated to highlight the significance of atmospheric pressure. It is shown that mass flow ratio ($m_{\text{ratio}} = \dot{m}_{w,in}/\dot{m}_a$) does not have any significant effect. Also, for rating calculations, it is noted that the efficiency increases with the mass flow rate ratio for both the evaporative cooler and condenser. It is noted that Webb [17] is correct in stating that the value of the tie-line would be constant in the evaporative condenser and that it would vary in the evaporative cooler. But it is found that, for a constant value of −11.1 of the tie-line, typically used in cooling towers is also valid for the evaporative cooler.


## Acknowledgements

The authors acknowledge the support provided by King Fahd University of Petroleum and Mineral throught the research project (ME/RISK-FOULING/230).

## Appendix A. Heat and mass transfer correlations

In this section, we present heat and mass transfer correlations that are relevant to the design and analysis of evaporative coolers and condensers.

The heat transfer coefficient during laminar flow ($Re<2300$) inside a duct with a constant wall temperature is given by [34]:

$$Nu_{\rm p} = 3.66 + \frac{0.104({\rm Re_p Pr_p}(d_{\rm t,in}/L))}{1 + 0.016({\rm Re_p Pr_p}(d_{\rm t,in}/L))^{0.8}} \tag{A.1}$$

The correlation for the heat transfer coefficient for a flow inside of a tube in a turbulent flow regime is obtained from Dreyer [6].

$$Nu_{\rm p} = \frac{(f_{\rm D}/8)({\rm Re_p} - 1000){\rm Pr_p}(1 + (d_{\rm t,in}/L)^{0.67})}{1 + 12.7(f_{\rm D}/8)^{0.5}({\rm Pr_p^{0.67}} - 1)} \tag{A.2}$$

where the friction factor $f_{\rm D}$ for smooth tubes was defined by

$$f_{\rm D} = (1.82\log_{10}{\rm Re_p} - 1.64)^{-2} \tag{A.3}$$

Eq. (A.2) is valid for the following ranges of Reynolds and Prandtl numbers

$$2300 < {\rm Re_p} < 10^6;\ 0.5 < {\rm Pr_p} < 10^4;\ 0 < \left(\frac{d_{\rm t,in}}{L}\right) < 1$$

Chato [35] proposed an equation that we used to determine the condensation heat transfer coefficient in essentially horizontal tubes and is only valid for relatively low vapor velocities ($Re<35{,}000$) at the tube inlet. This relationship is given by

$$h_{\rm r} = 0.555\left[\frac{g\rho_{\rm r,c}(\rho_{\rm r,c} - \rho_{\rm r,v})k_{\rm r,c}^3 h'_{\rm fg}}{\mu_{\rm r,c}(t_{\rm r} - t_{\rm wall})d_{\rm t,in}}\right]^{0.25} \tag{A.4}$$

with

$$h'_{\rm fg} = h_{\rm fg} + 0.68c_{\rm p,r}(t_{\rm r} - t_{\rm wall}) \tag{A.5}$$

Shah [36], however, predicted the same for higher vapor velocities,

$$h_{\rm r} = h_{\rm L}\left[0.55 + 2.09\left(\frac{P_{\rm cr}}{P_{\rm v}}\right)^{0.38}\right] \tag{A.6}$$

where $h_{\rm L}$ is given by

$$h_{\rm L} = 0.023{\rm Re_{r,c}^{0.8}Pr_{r,c}^{0.4}}\left(\frac{k_{\rm r,c}}{d_{\rm t,in}}\right) \tag{A.7}$$

The film heat transfer coefficient from outside of the tubes in a counterflow horizontal tube evaporative cooler are obtained from Mizushina et al. [8], which is also recommended by Dreyer [6]. It can be summarized as:

$$h_{\rm c,w} = 2102.9\left(\frac{\Gamma}{d_{\rm t,os}}\right)^{1/3} \tag{A.8}$$

with

$$0.195 < \left(\frac{\Gamma}{d_{\rm t,os}}\right) < 5.556 \tag{A.9}$$

where

$$\Gamma = \frac{\dot m_{\rm w,in} d_{\rm t,os}}{2n_{\rm tr}\widehat{P}_{t}L} \tag{A.10}$$

It is important to note that the correlation given by Mizushina et al. [8] was obtained from test data using tube diameters of 12.7, 19.05, and 40.0 mm.

The following volumetric correlation for the mass transfer coefficient was found to fit the test data of Mizushina et al. [8]:

$$h_{\rm D}a = 5.027\times10^{-8}({\rm Re_a})^{0.9}({\rm Re_w})^{0.15}(d_{\rm t,os})^{-2.6} \tag{A.11}$$

The interfacial area per unit volume of a tube bundle in a ($2\times d_{t,os}$) array can be expressed as

$$a = \frac{\pi d_{\rm t,os}}{(2d_{\rm t,os})(\sqrt{3}d_{\rm t,os})} = \frac{\pi}{(2\sqrt{3}d_{\rm t,os})} = \frac{0.9069}{d_{\rm t,os}} \tag{A.12}$$

The mass transfer coefficient based on interfacial area per unit volume of a tube bundle can now be simplified to

$$h_{\rm D} = 5.544\times10^{-8}({\rm Re_a})^{0.9}({\rm Re_w})^{0.15}(d_{\rm t,os})^{-1.6} \tag{A.13}$$

## References

[1] W. Goodman, The evaporative condenser, Heat Piping Air Cond 10 (1938) 165–328.

[2] E.G. Thomsen, Heat transfer in an evaporative condenser, Refrigeration Eng 51 (5) (1946) 425–431.

[3] D.D. Wile, Evaporative condenser performance factors, Refrigeration Eng 58 (1) (1950) 55–63 [see also 88–89].

[4] R.O. Parker, R.E. Treybal, The heat, mass transfer characteristics of evaporative coolers, AIChE Chem Eng Progr Symp Ser 57 (32) (1961) 138–149.

[5] W. Leidenfrost, B. Korenic, Evaporative cooling and heat transfer augmentation related to reduced condenser temperatures, Heat Transfer Eng 3 (3–4) (1982) 38–59.

[6] A.A. Dreyer, Analysis of evaporative coolers and condenser, MSc Thesis, University of the Stellenbosch, Rep. of South Africa, 1988.

[7] M. Poppe, H. Rögener, Evaporative cooling systems, VDI-Warmeatlas, Section Mh, 1984.

[8] T. Mizushina, R. Ito, H. Miyashita, Experimental study of an evaporative cooler, Int Chem Eng 7 (4) (1967) 727–732.

[9] T. Mizushina, R. Ito, H. Miyashita, Characteristics and methods of thermal design of evaporative coolers, Int Chem Eng 8 (3) (1968) 532–538.

[10] W. Zalewski, P.A. Gryglaszewski, Mathematical model of heat and mass transfer processes in evaporative fluid coolers, Chem Eng Proc 36 (1997) 271–280.

[11] W. Zalewski, Mathematical model of heat and mass transfer processes in evaporative condensers, Int J Refrigeration 16 (1993) 23–30.

[12] J.F. San José Alonso, F.J. Rey Martínez, E. Velasco Gómez, M.A. Alvarez-Guerra Plasencia, Simulation model of an indirect evaporative cooler, Energy Buil 29 (1998) 23–27.

[13] B. Halasz, A general mathematical model of evaporative cooling devices, Rev Gen Therm 37 (4) (1998) 245–255.

[14] I.C. Finlay, W.D. Grant, The accuracy of some simple methods of rating evaporative coolers, Report No. 584, National Engineering Laboratory, East Kilbride, Glasgow, 1974.

[15] S. Tezuka, T. Takada, S. Kasai, Performance of an evaporative cooler, Heat Transfer-Jpn Res 6 (1) (1976) 1–18.

[16] I.C. Finlay, W.D. Grant, Air coolers, cooling towers and evaporative coolers, Report No. 534, National Engineering Laboratory, East Kilbride, Glasgow, (1972) 165–328.

[17] R.L. Webb, A unified theoretical treatment for thermal analysis of cooling towers, evaporative condensers, and fluid coolers, ASHRAE Trans 90 (Part 2B) (1984) 398–415.

[18] R.L. Webb, A. Villacres, Algorithms for performance simulation of cooling towers, evaporative condensers, and fluid coolers, ASHRAE Trans 90 (Part 2B) (1984) 416–458.

[19] A.V. Bykov, V.A. Gogolin, N.V. Tovaras, Investigation of heat, mass transfer and fluid flow characteristics in evaporative condensers, Int J Refrigeration 7 (1984) 342–347.

[20] W. Zalewski, B. Niezgoda-Zelasko, M. Litwin, Optimization of evaporative fluid coolers, Int J Refrigeration 23 (2000) 553–565.

[21] X.C. Guo, T.S. Zhao, A parametric study of an indirect evaporative air cooler, Int Commun Heat Mass Transfer 25 (1998) 217–226.

[22] D.Q. Kern, R.E. Seaton, A theoretical analysis of thermal surface fouling, Br J Chem Eng 4 (5) (1959) 258–262.

[23] B.A. Qureshi, S.M. Zubair, The impact of fouling on performance evaluation of evaporative coolers and condensers, Int J Energy Research 29 (2005) 1313–1330.

[24] R.I. Macleod-Smith, How to control legionella without damaging your evaporative condenser, Presented at the 11th Annual Institute of Refrigeration Conference, London, 26th November, 2002.

[25] J.R. Khan, B.A. Qureshi, S.M. Zubair, A comprehensive design and performance evaluation study of counter flow wet cooling towers, Int J Refrigeration 27 (2004) 914–923.

[26] S.A. Klein, F.L. Alvardo, EES-Engineering Equation Solver. User's manual for Microsoft Windows Operating Systems, version 7.155, F-Chart Software, Madison, WI, 2001.

[27] H.M. Ettouney, H.T. El-Dessouky, W. Bouhamra, B. Al-Azmi, Performance of evaporative condensers, Heat Transfer Eng 22 (2001) 41–55.

[28] J.Y. Jang, Z.J. Wang, Heat and mass transfer performances of closed-type cooling towers, Proceedings of the International Conference on Advances in Computational Heat Transfer, Palm Cove, Queensland, Australia, May 20–25th, 2001. p. 269–276.

[29] Personal correspondence with Georges Hoeterickx of Baltimore Aircoil, 2004.

[30] I.C. Finlay, D. Harris, Evaporative cooling of tube banks, Int J Refrigeration 7 (4) (1984) 214–224.

[31] P.J. Erens, Comparison of some design choices for evaporative cooler cores, Heat Transfer Eng 9 (2) (1988) 29–35.

[32] J.W. Sutherland, Analysis of mechanical draught counter flow air/water cooling towers, ASME J Heat Transfer 105 (3) (1983) 576–583.

[33] D.R. Baker, H.A. Shryock, A comprehensive approach to the analysis of cooling tower performance, ASME Trans 83 (1961) 339–349.

[34] W.M. Kays, Numerical solution for laminar flow—heat transfer in circular tubes, Trans ASME 77 (1955) 1265–1274.

[35] J.C. Chato, Laminar condensation inside horizontal and inclined tubes, ASHRAE J (1962) 52–60.

[36] M.M. Shah, A general correlation for heat transfer during film condensation inside pipes, Int J Heat Mass Transfer 22 (1979) 547–556.